Development of Optically Interconnected LSI
−Integration of Ring Resonator Switches using Electro-Optic Materials−

Shin Yokoyama (Professor, Research Center for Nanodevices and Systems,
Graduate School of Advanced Sciences of Matter),
Yuichiro Tanushi (COE Researcher),
Masaru Wake (Graduate School of Advanced Sciences of Matter, M2),
Keita Wakushima (Faculty of Engineering, B4)

1. Research Target

With the progress of the miniaturization and switching speed of transistors, the performance of LSI is now governed by the signal transfer spe ed of the interconnection. Therefore, recently the RF wireless interconnection and optical interconnection are attracting much attention as a next generation interconnects in LSI instead of metal interconnection. In this twenty-first century COE program, the wireless interconnection and optical interconnection are studied. The author is in charge of the development of optical interconnection in LSI.

2. Research Results

The author has been studying optically interconnected LSI. We have so far developed three dimensional optically coupled common memory,[1] pattern recognition chip with optical interconnection,[2] and high-speed lift-off technique of light-emitting devices from GaAs substrate and the method to bond the lifted-off light-emitting devices onto Si LSI.[3] The achievements after this COE program started, are 1) development of stack-type branched waveguides with good light dividing controllability,[4] and 2) proposal of ring resonator switches using electro-optic materials, for which the refractive index is changed by the electric field.[5] In this paper item 2) is described.

2-1 Ring resonator switch using electro-optic materials

We have so far developed the integration technologies by bonding many light-emitting devices on Si chips.[3] However, this method is not so reliable and not suitable to the mass production. Instead of this, we propose a monolithic integration of optical switches,

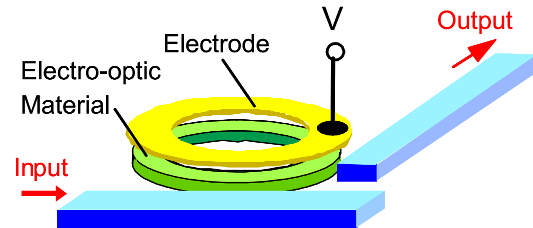

Fig. 2 Ring resonator switch using electro-optic material.

which modulate the light intensity. The schematic of the proposed optically interconnected LSI is shown in Fig. 1. For this purpose, we are studying optical switch using the optical micro-ring resonator,[6] which is recently attracting much attention. In our proposal, the electro-optic materials such as $LiNbO_3$ and $(Ba,Sr)TiO_3$, are used for the core layer of the ring resonator (Fig. 2). Then, the resonance wavelength can be changed by the applied bias voltage. Therefore, the optical switch using the ring resonator with the size of a few tens of microns can be realized by the structure shown in Fig. 2. The another type of tunable ring resonator by temperature control is reported by Kokubun *et al.*[7] However, the high-speed response is not expected by the temperature control method. On the other hand, the response frequency of the electro-optic material is expected to be tera-hertz order because the electro-optic effect is based on the ionic polarization. The speed of the actual devices is determined by the stray capacitance and the series resistance of the electrode.

Figure 3shows the cross section and the plan view of the ring resonator switch. The resonance wavelength λ is given by the following formula.

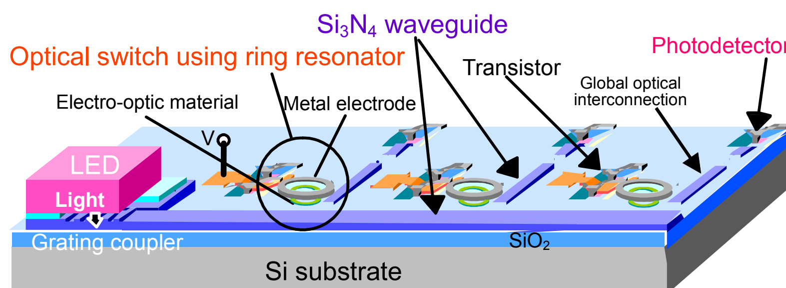

Fig. 1 Schematic of optically interconnected LSI proposed in this research rogram.

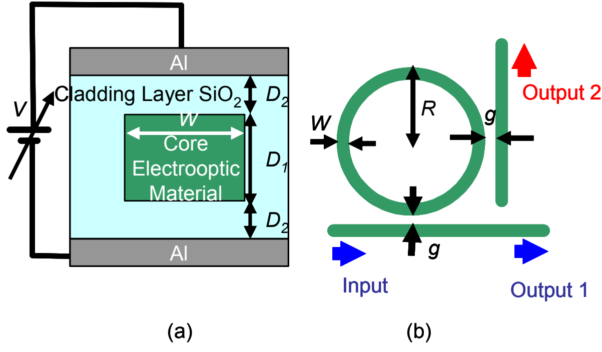

Fig. 3 (a) Cross section and (b) plan view of the ring resonator switch using electro-optic material.

$$\lambda = n_{eff}\frac{2\pi R}{m} \qquad (1)$$

Here, n_{eff} is the effective refractive index, R is the radius of the ring, and m is an integer. Figure 4 shows the simulated light propagation loss with the same cross section as in Fig. 3(a). The core is assumed to be $LiNbO_3$ with refractive index of 2.2 and the thickness is 0.5 µm. The two dimensional finite difference time-domain (FDTD) simulator (Apollo Photonic Solutions Suite) is used. The width of the waveguide is 2 µm, and the wavelength is 850 nm. From this figure, the thicker SiO_2 cladding layer than 0.25 µm is required to obtain a small propagation loss than 1 dB/cm. Such thick cladding layer leads to the higher operation voltage. In order to shrink the cladding layer, we have simulated the core thickness dependence of the propagation loss and the result is shown in Fig. 5. Here, the cladding layer is fixed at 0.1 µm. It is found that the core thicker than 3 µm results in small propagation loss less than 1 dB/cm. The thicker core film does not increase the operation voltage because the dielectric constant of the core film is usually large. Figure 6 shows the simulated resonance characteristics of the ring resonator with the ring radius of 12 µm, width of 2 µm, core ($LiNbO_3$) thickness of 0.5 µm, and cladding layer thickness of 0.1 µm. The gap width is 0.1µm. The electric field, E=3.1×10^{4}V/cm, induces the change in refractive index of 5×10^{-4}, which gives

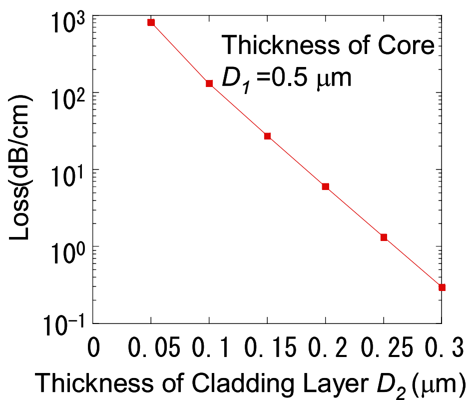

Fig. 4 Propagation loss versus thickness of cladding layer of the waveguide.

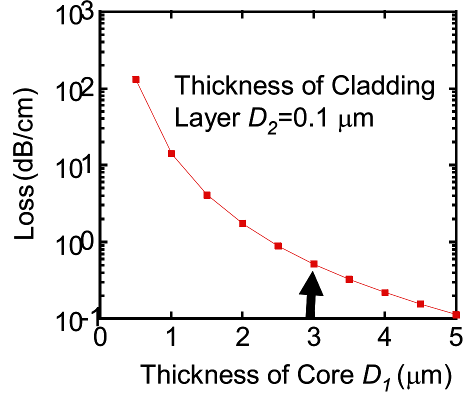

Fig. 5 Propagation loss versus thickness of core layer.

rise to the switching gain of 5 dB at wavelength of 852.35 nm. The switching operation voltage is given by the following formulae and is calculated to be 13.5 V.

$$\left.\begin{aligned} \Delta n &= -\frac{1}{2}n^3 rE \\ V &= D_{core}E + 2D_{SiO2}\frac{\varepsilon_{core}}{\varepsilon_{SiO2}}E \end{aligned}\right\} \qquad (2)$$

Here, n and Δn are, respectively, the refractive index of the core and its change due to the electric field, r is the electro-optic coefficient, D_{core} and D_{SiO2} are, respectively, thicknesses of the core and SiO_2 cladding layers, ε_{core} and ε_{SiO2} are, respectively, the dielectric constants of the core and cladding layers. The operation voltages and frequencies calculated for the various electro-optic materials are shown in Table 1 together with the characteristic constants. The operation frequency is calculated as the reciprocal time constant determined from the resistance and capacitance of the electrode (Al: 0.8 µm in thickness). The (Ba,Sr)TiO_3 film is studied for the DRAM application, however, the operation voltage is relatively high (92 V) due to the large dielectric constant. The improvement of the

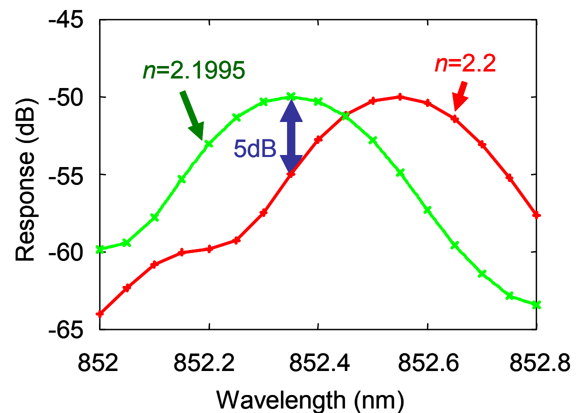

Fig. 6 Simulated response of output 2 in Fig. 3 for different refractive index of core layer.

Table 1 Operation voltage and frequency for ring resonator switches using various electro-optic materials.

	$LiNbO_3$	$(Ba,Sr)TiO_3$	$K(Ta,Nb)O_3$
Electro-optic Coefficient (pm/V)	30.8	23	600
Refractive Index n	2.2	2.1	2.35
Electric Field E (10^4 V/cm)	3.05	5	0.1284
Relative Dielectric Constant ε	28	300	28～300 (assumed)
Operation Voltage V (V)	13.5	91.9	0.57～2.36
Operation Frequency f (THz)	58	47	47～58

resonance sharpness (Q value) is required by, for example, devising the structure. Here, we have, for the first time, measured the electro-optic coefficient of the $(Ba,Sr)TiO_3$ film. The $K(Ta,Nb)O_3$,[8] which was recently developed by NTT results in the small operation voltages of a few V or less.

2-2 Fabrication and evaluation of ring resonator

First, we have developed the fabrication technology and evaluation method for the optical ring resonators. Plasma CVD Si nitride film was used for the core material. Figure 7 shows the developed measurement system. Figure 8 shows the measured resonance characteristics of the ring resonator of ring radius of 10 μm, waveguide width of 3 μm, and coupling gap width of 0.2 μm. The ring resonator was fabricated by electron beam lithography followed by the reactive ion etching of the Si nitride film. A good correlation between the dips in output1 and peaks in output2 is observed, which indicates that the resonance takes place and the resonated light power is transferred to the output2. Also a good agreement between the experimental and simulated results is observed.

2-3 Optical waveguide using electro-optic material

We have fabricated the optical waveguide using $(Ba,Sr)TiO_3$ (BST) film as a core material by spin coat method. The BST film was formed by spin coating the source liquid at an appropriate rotation speed and time, followed by the annealing at 550°C for 5 min. This sequence was repeated until the film thickness reaches the required value. The substrate is thermally oxidized SiO_2/Si substrate patterned by electron beam lithography and reactive ion etching as shown in Fig. 9(a), where the trenches are formed. After spin coating, the planarization takes place and the film thickness in the trench becomes thicker compared to the outside of the trench. Then, the light (He-Ne laser, 633 nm) is confined in the trench, which is shown in Fig. 9(b).

Figure 10 shows the measured propagation loss as a function of the width of the trench. It is noted that for the thicker core film (d=0.3 μm) the propagation loss is larger than that of the thinner one (d=0.2 μm) in the narrow trench region (<28 μm). This is interpreted as follows. As the core film becomes thicker, the film thickness outside the trench region also becomes

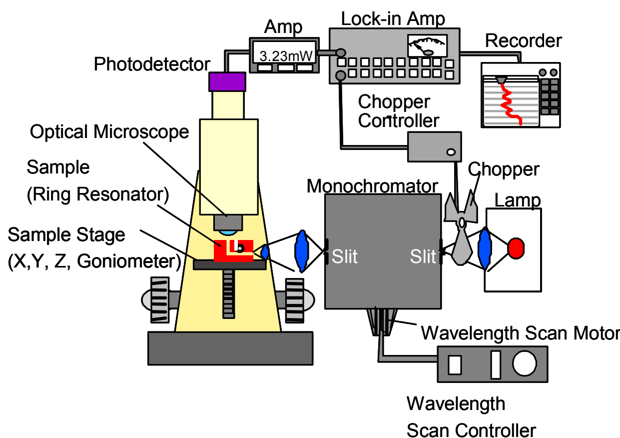

Fig. 8 Resonance characteristics of fabricated ring resonator with Si nitride core.

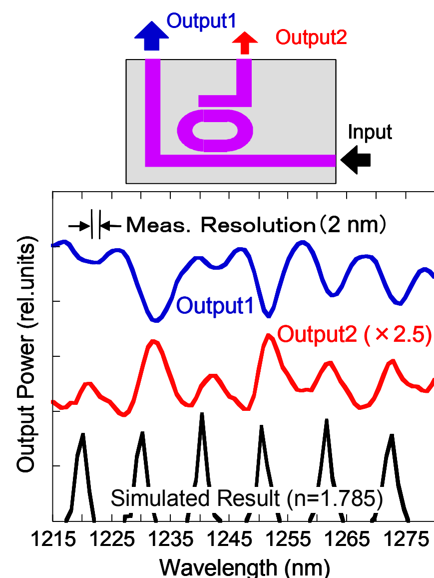

Fig. 7 Measurement system for optical ring resonators.

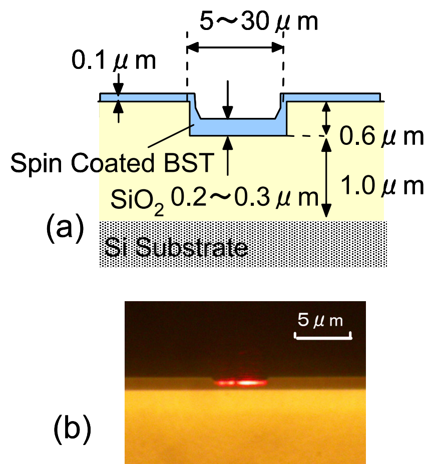

Fig. 9 (a) Cross section of fabricated trench type optical waveguide and (b) optical micrograph of the output light.

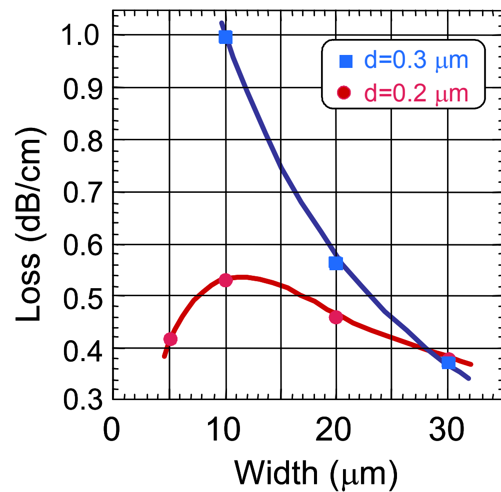

Fig. 10 Light propagation loss for the fabricated waveguide with electro-optic material core.

thicker. Therefore, the light confinement in the trench is weakened.

3. Summary

The ring resonator switch using electro-optic material is proposed and its properties are simulated. As a result, operation voltage is estimated for the several electro-optic materials. The design, fabrication and measurement technologies for the ring resonators with Si nitride core are developed. We have fabricated the optical waveguide using the electro-optic material of $(Ba,Sr)TiO_3$, and the light propagation loss was measured.

4. Future Plan

The ring resonator switch using electro-optic material will be fabricated and measured. The subject to be solved is to improve the crystal quality of the film by adjusting the annealing temperature, to increase the quality factor (Q) of the ring resonator by modifying the resonator structure, and to decrease the operation voltage.

References

1) K. Miyake *et al.*, Jpn. J. Appl. Phys. **34**(1995)1246.

2) T. Doi *et al.*, Jpn. J. Appl. Phys. **35** (1996) 1405.

3) Y. Sasaki *et al.*, J. Electrochem. Soc. **146**(1999)710.

4) Y. Hara *et al.*, Optical Review **10**(2003) 357.

5) Y. Tanushi *et al.*, Ext. Abst. (The 51st Spring Meeting 2004); The Japan Society of Applied Physics and Related Societies, 29a-ZC-9 [in Japanese].

6) B. E. Little *et al.*, J. Lightwave Technol. **15** (1997) 998.

7) Y. Kokubun, Oyo Buturi **72** (2003) 1364 [in Japanese].

8) K. Fujiura *et al.*, NTT Tech. J. (2004)56.

Achievements

Optical Interconnection

(Journal)

1) Y. Hara, S. Yokoyama and K. Umeda, “Compact Branched Optical Waveguides Using High-Index-Contrast Stacked Structure,” Optical Review 10, No. 5, pp. 357-360 (2003).

(Proceedings)

2) Y. Tanushi, M. Wake and S. Yokoyama, “Race－Track Optical Ring Resonators with Groove Coupling,” submitted to Int. Conf. on Solid Stare Devices and Materials (SSDM2004).

3) Y. Tanushi, M. Wake. K. Wakushima, M. Suzuki and S. Yokoyama, “Technology for Ring Resonator Switches using Electro-Optic Materials,” submitted to 1st Int. Conf. On Group IV Photonics (2004).

Scaled Devices

(Journal)

1) T. Yoshino *et al.*, "Influence of Organic Contaminant on Trap Generation in Thin SiO_2 of Metal-Oxide-Semiconductor Capacitors": Jpn. J. Appl. Phys. **41**(2002)4750.

2) K. Kawamura *et al.*, “Coulomb blockade effects and conduction mechanism in extremely thin polycrystalline-silicon wires,” J. Appl. Phys. Lett. **91**(2002)5213.

3) Shin Yokoyama *et al.*, "Influence of Wafer Storage Environment on MOS Device Characteristics," J. Aerosol Research, Japan **17**(2002)96 [in Japanese].

4) M. Kohno *et al.*, “Evaluation of Surface Contamination by Noncontact Capacitance Method under UV Irradiation,” Jpn. J. Appl. Phys. **42**(2003)5837.

5) M. Kohno *et al.*, “Investigation of Surface Contamination on Silicon Oxide after HF Etching by Noncontact Capacitance Method,” Jpn. J. Appl. Phys. **42**(2003) 7601.

6) Q.D.M. Khosru *et al.*, “Organic Contamination Dependence of Process Induced Interface Trap

Generation in Ultrathin Oxide Metal Oxide Semiconductor Transistors," Jpn. J. Appl. Phys. **42**(2003)L1429.

7) H. Setyawan *et al.*, "Particle Formation and Trapping Behavior in a TEOS/O_2 Plasma and Their Effects on Contamination of a Si Wafer," Aerosol Science and Technology **38**(2004)120.
8) M. Ooka *et al.*, "Excellent Contact-Hole Etching with NH_3 Added C_5F_8 Pulse-Modulated Plasma," Jpn. J. Appl. Phys. **43**(2004) (in press).

(Proceedings)

9) M. Ooka *et al.*, "Ultrasmall SiO_2 Hole Etching using PFC Alternative Gas with Small Global Greenhouse Effect," Digest of Pacific Rim Workshop on Transducers and Micro/Nano Technologies (MEMS2002) (2002) pp. 111-114.
10) M. Kohno *et al.*, "Evaluation of Surface Contamination by Noncontact Capacitance Method under UV Irradiation," Extend. Abst. Int. Conf. on Solid State Devices and Materials (SSDM2002) (2002) pp. 724-725.
11) M. Ooka *et al.*, "Excellent Contact-Hole Etching with NH_3 Added C_5F_8 Pulse-Modulated Plasma," Extend. Abst. Int. Conf. on Solid State Devices and Materials (SSDM2003) (2003) pp. 454-455.
12) M. Suzuki and S. Yokoyama, "Anomalous Behavior of Interface Traps of Si MOS Capacitors Contaminated with Organic Molecules," submitted to Int. Conf. on Solid State Devices and Materials (SSDM2004).
13) T. Kakite and S. Yokoyama, "Characterization of Porous Silicon Nitride Formed by Plasma-Enhanced Chemical Vapor Deposition," submitted to 206th Meeting of The Electrochemical Society (2004).